Atmos. Chem. Phys., 22, 7619–7630, 2022
https://doi.org/10.5194/acp-22-7619-2022

Atmospheric Chemistry and Physics
Open Access
EGU

Research article

The chemical composition and mixing state of BC-containing particles and the implications on light absorption enhancement

Jiaxing Sun[1,2], Yele Sun[1,2,3], Conghui Xie[1,2,a], Weiqi Xu[1], Chun Chen[1,2], Zhe Wang[1], Lei Li[4], Xubing Du[4,5], Fugui Huang[6], Yan Li[1,2], Zhijie Li[1,2], Xiaole Pan[1], Nan Ma[7], Wanyun Xu[8], Pingqing Fu[9], and Zifa Wang[1,2,3]

[1]State Key Laboratory of Atmospheric Boundary Layer Physics and Atmospheric Chemistry, Institute of Atmospheric Physics, Chinese Academy of Sciences, Beijing 100029, China
[2]College of Earth and Planetary Sciences, University of Chinese Academy of Sciences, Beijing 100049, China
[3]Center for Excellence in Regional Atmospheric Environment, Institute of Urban Environment, Chinese Academy of Sciences, Xiamen 361021, China
[4]Institute of Mass Spectrometry and Atmospheric Environment, Jinan University, Guangzhou 510632, China
[5]Guangdong Provincial Engineering Research Center for On-Line Source Apportionment System of Air Pollution, Guangzhou 510632, China
[6]Guangzhou Hexin Analytical Instrument Company Limited, Guangzhou 510530, China
[7]Institute for Environmental and Climate Research, Jinan University, Guangzhou 511443, China
[8]State Key Laboratory of Severe Weather & Key Laboratory for Atmospheric Chemistry, Institute of Atmospheric Composition, Chinese Academy of Meteorological Sciences, Beijing 100081, China
[9]Institute of Surface-Earth System Science, Tianjin University, Tianjin 300072, China
[a]now at: State Key Joint Laboratory of Environmental Simulation and Pollution Control, College of Environmental Sciences and Engineering, Peking University, Beijing 100871, China

Correspondence: Yele Sun (sunyele@mail.iap.ac.cn)

Received: 29 October 2021 – Discussion started: 26 November 2021
Revised: 25 May 2022 – Accepted: 30 May 2022 – Published: 13 June 2022

Abstract. The radiative forcing of black carbon (BC) depends strongly on its mixing state in different chemical environments. Here we analyzed the chemical composition and mixing state of BC-containing particles by using a single-particle aerosol mass spectrometer and investigated their impact on light absorption enhancement (E_{abs}) at an urban (Beijing) and a rural site (Gucheng) in the North China Plain. While the BC was dominantly mixed with organic carbon (OC), nitrate, and sulfate at both the urban and rural sites, the rural site showed a much higher fraction of BC coated with OC and nitrate (36 % vs. 15 %–20 %). Moreover, the BC mixing state evolved significantly as a function of relative humidity (RH), with largely increased coatings of OC–nitrate and nitrate at high RH levels. By linking with an organic aerosol (OA) composition, we found that the OC coated on BC comprised dominantly secondary OA in Beijing, while primary and secondary OA were similarly important in Gucheng. Furthermore, E_{abs} was highly dependent on secondary inorganic aerosol coated on BC at both sites, while the coated primary OC also resulted in an E_{abs} of ~ 1.2 for relatively fresh BC particles at the rural site. A positive matrix factorization analysis was performed to quantify the impact of different mixing states on E_{abs}. Our results showed a small E_{abs} (1.06–1.11) for BC particles from fresh primary emissions, while the E_{abs} increased significantly above 1.3 when BC was aged rapidly with increased coatings of OC–nitrate or nitrate; it can reach above 1.4 as sulfate was involved in BC aging.

1 Introduction

Black carbon (BC), also referred to as soot or elemental carbon, contributes a substantial and positive impact on climate radiative forcing (Bond et al., 2013; IPCC, 2013). The high loading of atmospheric BC could depress the development of the planetary boundary layer and aggravate haze pollution episodes (Ding et al., 2016). However, accurate estimations of light absorption and radiative forcing of BC are still challenging due to its complex emission sources (e.g., fossil fuel and biomass burning) and microphysical properties (e.g., mixing state and coating composition) (Kahnert, 2010; Vignati et al., 2010; Liu et al., 2017; Cappa et al., 2019; Sun et al., 2022). Light absorption of BC is composed of pure BC absorption and enhanced light absorption (E_{abs}) induced by a "lensing effect", which is due to the chemical materials coated on BC (Fuller et al., 1999; Bond and Bergstrom, 2006; Lack and Cappa, 2010). In order to determine the E_{abs}, the thermodenuder (TD) method (Liu et al., 2015; Zhang et al., 2016), mass absorption efficiency (MAE) method (Wang et al., 2014; Zhang et al., 2018), and Mie theoretical calculations (Liu et al., 2017) are widely used in previous studies. However, the E_{abs} in different chemical environments is considerably different, such as the negligible E_{abs} (1.06) in California versus a significant light absorption enhancement (~ 1.8) in Kanpur (Cappa et al., 2012; Thamban et al., 2017). One explanation is due to the variety of the mixing states of BC from different sources, urban and rural background sites, and aging processes (Liu et al., 2015, 2017, 2020).

Extensive studies have been conducted to characterize the mixing state of BC (W. J. Li et al., 2016). Buseck et al. (2014) used transmission electron microscopy (TEM) to determine the size, morphology, mixing state, and chemical compositions of soot particles, and W. Li et al. (2016) used the same technique for the characterization of the size and aging dependent mixing state of individual particles in both clean and polluted environments in China. More recently, the development of the soot-particle aerosol mass spectrometer (SP-AMS) can measure refractory BC (rBC) and coated aerosol species in real time (Lee et al., 2015). For example, Xie et al. (2019a) found that secondary organic and inorganic components contributed mostly to the coating materials of rBC in summer, while Liu et al. (2019a) reported that rBC was more mixed with primary organic components (e.g., coal combustion and biomass burning) than secondary species in winter. Comparatively, a more comprehensive mixing state of BC particles and the chemical compositions of coatings could be acquired by aerosol time-of-flight mass spectrometry (ATOFMS) or single-particle aerosol mass spectrometry (SPAMS) (Pratt and Prather, 2012). Recent studies in winter in the North China Plain (NCP) showed that most BC particles were mixed with sulfate and organic carbon (OC) due to the intensive coal combustion and biomass burning emissions in the heating period (Y. Chen et al., 2020a; Wang et al., 2020), while BC particles were more mixed with nitrate in summer in Beijing (Xie et al., 2020). Although the mixing state, coating compositions, and E_{abs} of BC have been widely discussed in previous studies, our understanding of BC properties in winter, particularly the differences between urban and rural areas in the NCP, is limited.

In this study, we deployed a newly developed high-resolution single-particle aerosol mass spectrometer (Zhu et al., 2020), and a photoacoustic extinctiometer (PAX) coupled with a thermodenuder at an urban and a rural site in the NCP to investigate the mixing state of BC-containing particles and its relationship with light absorption enhancement. Meanwhile, the aerosol bulk composition was measured simultaneously by a high-resolution aerosol mass spectrometer (HR-AMS). The chemical composition and mixing state of BC-containing particles are characterized, and the evolution of the BC mixing state and the driving factors are investigated. Finally, the impacts of the changes in the mixing state of BC on light absorption enhancement and radiative forcing are elucidated.

2 Methods

2.1 Sampling sites and measurements

The measurements were conducted at an urban site from 18 October to 1 December 2019, and a rural site from 9 December 2019 to 13 January 2020. The urban site is located at the Institute of Atmospheric Physics (IAP), Chinese Academy of Sciences (39°58′28″ N, 116°22′16″ E) in Beijing (BJ). The rural site of Gucheng (GC) in the Hebei province is located ~ 120 km to the southwest of Beijing. Ambient aerosols with a flow rate of $3\,L\,min^{-1}$ were drawn into a $PM_{2.5}$ cyclone (Model: URG-2000-30ED) and a Nafion dryer. Then, aerosol particles ($\sim 2\,L\,min^{-1}$) were sampled by switching between a thermodenuder (TD) and a bypass line (BP) every 15 min into a HR-AMS to measure non-refractory submicron aerosol (NR-PM_1) species, and a PAX (Droplet Measurement Technologies) for absorption [$b_{abs}(\lambda)$] and scattering [$b_{sca}(\lambda)$] coefficients at 870 nm. Note that equivalent BC (eBC) is converted from $b_{abs}(\lambda)$ into mass concentration with a reference mass absorption efficient (MAE_{ref}, $4.44\,m^2\,g^{-1}$ in this study) (Bond and Bergstrom, 2006). A complete TD cycle took 150 min, during which the temperature increased gradually from 25 to 250 °C, followed by a 15 min cooling down to 25 °C. To minimize the uncertainties due to the changes during the measurements of TD and bypass, the $b_{abs,\,total}$ was obtained from the linear interpolation of measured ambient absorptions adjacent to the TD time; the E_{abs} was then determined as the ratio of $b_{abs,\,total}$ to $b_{abs,\,BCpure}$ that was defined as the thermodenuded particle absorption in the TD line at $T > 200°$. Note that we did not do a TD loss correction in this study. The reason is that the underestimated E_{abs} of $\sim 14\,\%$ due to the TD loss (Fig. S1 in the Supplement) can be relatively offset by the overestimation of $\sim 16\,\%$ due to the coating materials that did not evaporate at 210° (Ma et al., 2020; Xu et al., 2021a). More detailed descriptions of the measurements and methods can be found in our previous study (Sun et al., 2021).

A high-resolution single-particle aerosol mass spectrometer (HR-SPAMS, Hexin Instrument Co., Ltd.) was deployed independently in the same room to detect the mixing state and chemical composition of single particles in the ambient atmosphere. The aerodynamic diameters of single particles are determined from the velocity detected by two continuous laser beams (diode Nd:YAG, 532 nm). After passing through the sizing region, particles are desorbed and ionized by a pulsed Nd:YAG laser (266 nm), and the positive and negative fragments are detected by a Z-shaped bipolar time-of-flight mass spectrometer to obtain the chemical compositions. A more detailed description of the SPAMS can be found elsewhere (Li et al., 2011). Compared with the traditional SPAMS, the new HR-SPAMS uses a new aerosol concentration sampling device and improves the transmission efficiency of coarse particles. Meanwhile, a delayed extraction technology is introduced to improve mass resolution and increase the hit rate by a factor of 2–4 for ambient particles (Y. Chen et al., 2020b). Also, the ion signals with high and low intensity are separated by multichannel acquisition technology and detected simultaneously, which makes the system's dynamic range more than 40 times the traditional data acquisition system and greatly improves the detection of ions with low signals (Shen et al., 2018; Zhong et al., 2021).

2.2 Data analysis

In total, 3 619 038 and 4 655 426 particles were analyzed in BJ and GC, respectively. The size and chemical composition of each single particle is informed by the Computational Continuation Core (COCO) toolkit in the MATLAB software. Based on the marker of $C_n^{\pm}$ ($n = 1, 2, 3\ldots$) clusters, 2 269 659, and 3 399 565 BC-containing particles were identified in BJ and GC, respectively. Four typical sources of BC-containing particles are further identified according to the characteristic ion markers: (1) particles containing abundant signals of $39[K]^+$, $45[CHO_2]^-$, and $59[C_2H_3O_2]^-$ or $73[C_3H_5O_2]^-$, with peak areas of more than 0.5 % are classified as BB_{pure} type from biomass burning (Silva et al., 1999; Healy et al., 2010); (2) particles containing abundant signals of $7[Li]^+$, $23[Na]^+$, $27[Al]^+$, $43[AlO]^-$, $80[SO_3]^-$, $97[HSO_4]^-$, and polycyclic aromatic hydrocarbons are classified as CC_{pure} type from coal combustion (Zhang et al., 2009; Healy et al., 2010); (3) particles containing abundant signals of $40[Ca]^+$, $51[V]^+$, $55[Mn]^+$, $67[VO]^+$, $46[NO_2]^-$, $62[NO_3]^-$, and $79[PO_3]^-$ are classified as TR_{pure} type from traffic emissions (Yang et al., 2017); and (4) particles internally mixed with more than one source (the three sources mentioned above) are unified and named Mix_{Source} type. The BC-containing particles above are collectively referred to as BC_{fresh}. The remaining BC-containing particles are named BC_{aged} and classified using the ART-2a algorithm with a vigilance factor of 0.75, a learning rate of 0.05, and 20 iterations (Song et al., 1999). Seven particle types are grouped and named based on two principles: (1) the particles are named BCOC when the signals of $37[C_3H]^+$, $43[C_2H_3O]^+$, $51[C_4H_3]^+$, and $63[C_5H_3]^+$ are comparable with C_n^+ in the positive ion area (Healy et al., 2012; Xie et al., 2020), otherwise, they are named BC; and (2) on the basis of (1), the particles are named $BCOC_N$ or $BCOC_S$ when they are only mixed significantly with nitrate ($46[NO_2]^-$ and $62[NO_3]^-$), or sulfate ($97[HSO_4]^-$). Otherwise, they are named $BCOC_{NS}$ when they present comparable peak areas of nitrate and sulfate. The more detailed names of BC-containing particle types are given in Table S1 in the Supplement. According to previous studies, the coating materials on BC-containing particles measured by SPAMS refer to chemical components that are partially or fully coated on BC (Bond and Bergstrom, 2006; Healy et al., 2012; Pratt and Prather, 2012; Bi et al., 2015; Chen et al., 2016; Xie et al., 2020).

The sources of bulk organic aerosol (OA) from HR-AMS measurements were analyzed by positive matrix factorization (PMF). Five OA factors were identified at both urban and rural sites, including biomass burning OA (BBOA), fossil fuel-related OA (FFOA), cooking OA (COA), less oxidized oxygenated OA (LO-OOA) and more oxidized OOA (MO-OOA) in Beijing and BBOA, coal combustion OA (CCOA), hydrocarbon-like OA (HOA), OOA, and aqueous-related OOA (aq-OOA) in GC. The detailed PMF analyses of OA in Beijing and Gucheng are presented by Xu et al. (2021b) and Chen et al. (2022). The PMF analysis was also performed to identify the effect of different mixing states on E_{abs} by inputting $b_{abs,\,total}$, $b_{abs,\,BCpure}$, and 11 major types of BC-containing particles derived from HR-SPAMS. The detailed pre-treatment of the error matrix (in the Supplement) and the selection of factor solutions can be found in previous studies (Petit et al., 2014; Xie et al., 2019b). Then, the E_{abs} of each factor can be calculated as the ratio of $b_{abs,\,total,\,f_i}$ and $b_{abs,\,BCpure,\,f_i}$ in factor i.

3 Results and discussion

3.1 BC-containing particles at urban and rural sites

The BC-containing particles accounted for 62 % of the total particles in BJ; lower than in GC (73 %), yet higher than in winter Beijing 2018 (55 %) (Xie et al., 2020), likely due to the higher mass fraction of eBC in this study (9.3 % vs. 6.1 %). Similarly, a previous winter study in Beijing also found that 60 %–78 % of the aerosol particles contained BC (L. Chen et al., 2020). According to Figs. 1 and S2, we found that the mass spectra of the BC-containing particles at the two sites are somewhat similar. Both are characterized by $C_n^{\pm}$ ($n = 1$–7), $27[C_2H_3]^+$, $37[C_3H]^+$, $43[C_2H_3O]^+$, $51[C_4H_3]^+$ $63[C_5H_3]^+$, $46[NO_2]^-$, $62[NO_3]^-$, and $97[HSO_4]^-$ peaks, indicating that the BC-containing particles are consistently mixed with OC, nitrate (NO_3), and sulfate (SO_4) at the rural and urban sites. Comparatively, more than 80 % of the BC-containing particles were internally mixed with SO_4 in BJ, while those in GC accounted for less than 60 %. Considering the higher relative area of the secondary organic fragment of $43[C_2H_3O]^+$ (Healy et al., 2010; Chen et al., 2019) in BJ (Fig. 1), we concluded that the BC particles were likely more aged at the urban site. Another support is the much lower primary emissions of biomass burning and coal combustion in BJ than GC (Sun et al., 2020). In addition, approximately 40 % of the BC-containing particles were mixed with amines (e.g., $59[(CH_3)_3N]^+$ and $74[(C_2H_5)_2NH_2]^+$) in GC, which was twice that in BJ. One explanation is that the more nitrogen-containing compounds formed from either aqueous-phase processing due to higher RH (69 % vs. 45 %), or biomass-burning emissions at the rural site (Zhang et al., 2012; Chen et al., 2019).

The study in Beijing was divided into two periods: the non-heating period (BJ-NHP) from 28 October to 10 November and the heating period (BJ-HP) from 10 November to 1 December. The observation in GC was performed during the heating period. As illustrated in Fig. 2a, the BC-containing particles are dominantly contributed by BC_N and $BCOC_N$ ($\sim$ 20 %) during BJ-NHP, indicating that BC was mainly internally mixed with nitrate at the urban site. Compared with BJ-NHP, the fractions of $BCOC_S$ and Mix_{Source} increased significantly during BJ-HP, especially during relatively clean periods. This suggests a considerable change in the BC mixing state from the non-heating to the heating period due to the enhanced primary emissions, e.g., coal combustion. Previous studies showed that BC was mainly mixed with sulfate in winter in Beijing (Y. Chen et al., 2020a; Xie et al., 2020), while this study showed a dominant mixing of BC with nitrate. This was likely due to the fact that coal fuel in Beijing was replaced with clean energy, e.g., natural gas and electricity, after 2017 (Zhang et al., 2019). Indeed, the changes in nitrate concentrations were relatively small in winter in Beijing, since clean air action although the sulfate concentrations showed large decreases (Zhou et al., 2019; Lei et al., 2020). Comparatively, $BCOC_N$ was the major BC-containing particle type accounting for 36 % in GC, which was twice that in BJ-HP, indicating that BC particles were dominantly mixed with OC and nitrate in an environment with high RH and intensive primary emissions, e.g., coal combustion emissions. In addition, BB_{pure} and TR_{pure} showed pronounced diurnal cycles in GC (Fig. S3) compared with the relatively flat diurnal variations of BB_{pure} in BJ, suggesting intensive biomass burning and diesel vehicle emissions at the rural site, especially at nighttime.

3.2 Chemical composition and mixing states in different environments

Figure 3 shows the variations of number fractions of different BC-containing types under different RH levels in BJ and GC. Almost all BC_{aged} types showed strong dependence on RH, while the number fractions of BC_{fresh} types decreased with increasing RH at both sites, indicating that a high RH environment was more favorable for BC aging (Zhang et al., 2021). Similar to BC_{fresh}, $BCOC_S$ was the only type of aged BC showing a decreased fraction as a function of RH in BJ and GC. In fact, the higher number fraction of $BCOC_S$ during the clean period highlights that the relatively fresh BC could be directly mixed with OC and SO_4 at a low RH level, and evolved towards mixing with OC and NO_3 under high RH conditions. Moreover, the number fraction of BC_N increased gradually with the increase of RH, and dominated BC particles (25 %–30 %) at RH = 70 %–100% in BJ. Considering the similar increases of PM ($NR\text{-}PM_1$ + eBC) as a function of RH (Figs. 3a and S4), the RH dependence of BC_N suggested that the newly formed nitrate coating fresh BC played an important role in the formation of severe pollution in the urban region. Comparatively, the number fraction of $BCOC_N$ increased the most by 43 %, accounting for more than half of the BC-containing particles at high RH and PM levels in GC. This result indicates that the type of $BCOC_N$ was more important to aggravate air pollution in the rural area, being supported by the relatively high correlation between the number fraction of $BCOC_N$ and PM (Fig. S4). In addition, $BCOC_{NS}$ was likely affected by the photochemical production in GC, which is supported by the significantly increased number counts and fraction of $BCOC_{NS}$ during the daytime (Fig. S3). We found that the fraction of $BCOC_{NS}$ decreased obviously as a function of RH in GC, indicating the impact of the transition from photochemical production to aqueous-phase reactions on the mixing state of BC. Considering the increased SO_4 mass fraction, yet the relatively stable E_{abs} at RH > 70 % (Sun et al., 2021), we inferred that the aqueous-phase formation of sulfate at a high RH level appeared not to affect the BC mixing state substantially, consistent with a previous study (Zhang et al., 2021). However, $BCOC_{NS}$ in BJ showed relatively stable fractions across different RH levels, suggesting the different sources from the rural site.

Figure 3c and d show the evolution of the mixing state of BC-containing particles during two different haze events in BJ. During the initial stage of haze Case 1 (P0, Fig. 3c), the contribution of $BCOC_S$ started to decrease, while the number fraction of $BCOC_N$ increased significantly. As a consequence, E_{abs} increased rapidly from $\sim$ 1.1 to 1.3 in half a day. Then, the number fraction of BC_N increased while that of BC_{fresh} decreased during the P1 period. These results indicated that fresh BC was gradually aged by mixing with nitrate during the evolution of the haze episode. BC_N increased continually during P2 with E_{abs} up to 1.4, and finally, the mixing state of BC was stabilized as indicated by the relatively stable number fractions of most BC particle types and small changes in E_{abs}. Similar to haze Case 1, BC was mixed with nitrate and OC causing a high E_{abs} (up to 1.5) during P3 and P4 (Fig. 3d). As shown in Figs. 3d and S5, the sources

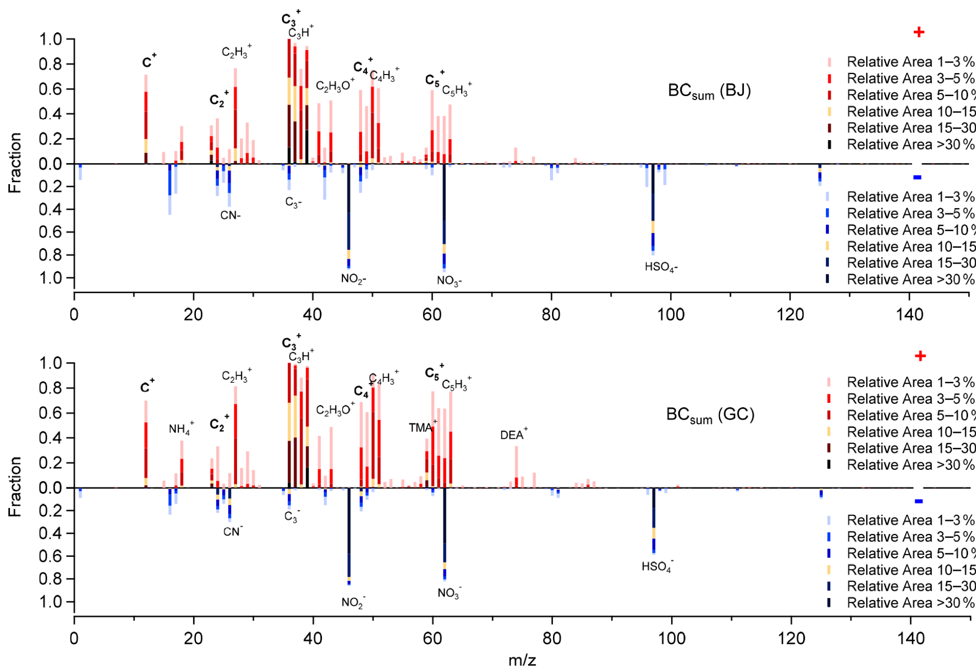

Figure 1. Digital positive and negative mass spectra of BC-containing particles in Beijing and Gucheng. The ion height indicates its number fraction in the BC-containing dataset (i.e., the number ratio of BC-containing particles with the corresponding ion detected in the mass spectra to the total BC-containing particles). The color bars represent each relative peak area corresponding to a specific fraction in the individual particles.

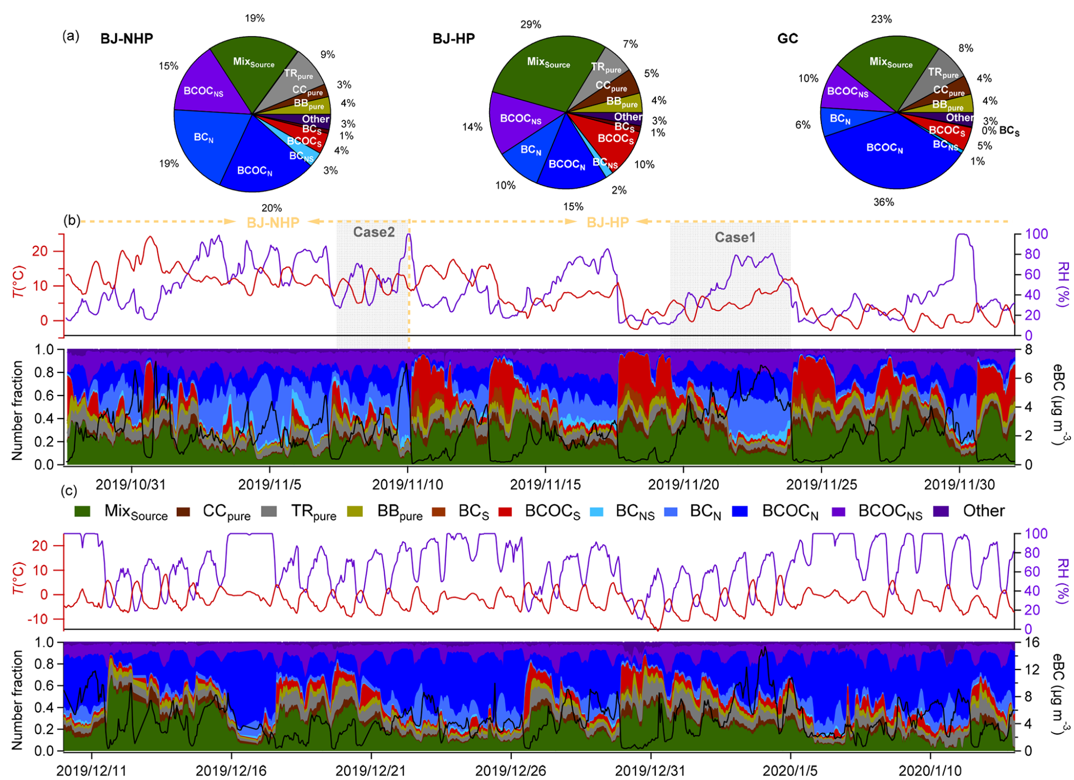

Figure 2. (a) Relative number abundance distribution of major BC-containing particle types during different periods. Temporal variation of ambient temperature (T), relative humidity (RH), and number fractions of BC-containing particle types in **(b)** Beijing and **(c)** Gucheng.

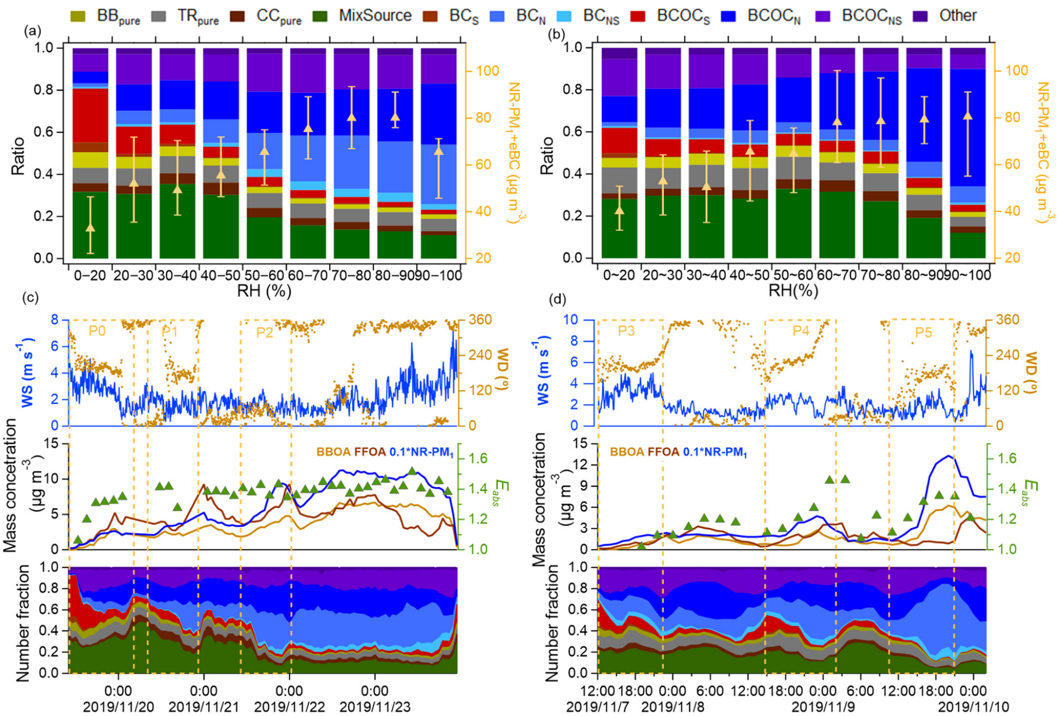

Figure 3. Variations of number fractions of BC-containing particle types with RH in **(a)** Beijing and **(b)** Gucheng. The bottom and top error bars represent the 25th and 75th percentiles. Temporal variations of wind speed (WS), wind direction (WD), E_{abs}, number fractions of BC-containing particle types, and mass concentrations of species during pollution of **(c)** Case 1 and **(d)** Case 2 in Beijing.

of fine particles were dominated by fossil fuel OA and presented strong diurnal variations consistent with changes in wind direction due to the influences of mountain valley winds (Sun et al., 2016). As a result, E_{abs} also presented a relatively consistent variation with FFOA and showed higher values at nighttime, indicating that the different chemical composition and mixing state associated with the changes in air masses due to the mountain valley winds had affected the light absorption enhancement of BC (Ding et al., 2021). The number fraction of BC_N increased significantly during the severest polluted period (P5) associated with simultaneous increases in BBOA, indicating the mixing of BC from biomass burning with nitrate under high RH and PM levels. Hence E_{abs} was comparably high (1.35). After the P5 period (from 21:00 on 9 November to 00:00 on 10 November, Beijing standard time), the BBOA decreased slightly and FFOA increased significantly. The proportion of $BCOC_N$ in BC was correspondingly higher. A similar variation could also be found during 14:00–19:00 on 8 November. These results indicated that BC emitted from fossil fuel emissions was likely mixed with OC and nitrate at a high PM level. Different from Beijing, the evolution of the BC mixing state was similar during most of the haze events in GC (Figs. S3 and 2c), which was generally characterized by a more significant increase in $BCOC_N$ than BC_N. Moreover, $BCOC_N$ particles increased more significantly during the nighttime, while $BCOC_{NS}$ was more significant during the daytime. These differences were mainly due to the enhanced coal combustion pollutants during the nighttime (Fig. S3), which were mixed with photochemical products during the daytime.

Overall, our results suggest that the fresh BC particles from biomass-burning emissions are more directly mixed with nitrate under high RH conditions, and then mixed with more sulfate during further aging. Comparatively, the fresh BC particles from coal combustion are often mixed with OC and sulfate first, and then mix further with OC and nitrate at high a RH level. In addition, our results also demonstrate that the E_{abs} in GC was largely due to coal combustion emissions internally mixed with OC, consistent with our previous study showing the large impact of coal combustion emissions on E_{abs} (Sun et al., 2021).

3.3 Effects of chemical composition on E_{abs}

As shown in the average positive mass spectra of the total BC-containing particles (Fig. S2), the peak areas of C_n^+, OC, and metal contributed more than 95 % to the total peak area, while the peak areas of NO_3 ($46[NO_2]^-$ and $62[NO_3]^-$) and SO_4 ($97[HSO_4]^-$) accounted for more than 80 % in the negative mass spectra. To better characterize the relationship between the chemical species and E_{abs}, we summed the $C_n^\pm$ ($n = 1$–5, accounting for more than 99 % in C_n) peak areas to represent BC and the total of NO_3 and SO_4 peak areas to represent the secondary inorganic components coated on BC. In addition, the sum of the positive peak areas, except C_n^+, was defined as OC + Metal to represent the OC and metal components coated on BC. These peak areas covered almost all of the chemical components coated on BC in the total BC-containing particles.

Figure 4a and b show the relationship between the peak area ratios (measured by HR-SPAMS) and the mass concentration ratios (measured by HR-AMS) in BJ and GC, respectively. With the increase of $(NO_3 + SO_4)_{AMS}$ / eBC mass concentration ratio, the $(NO_3 + SO_4) / C_n$ peak area ratio increased first and then gradually became stable at both sites. These results indicated that BC was rapidly aged and internally mixed with secondary inorganic components during the early stage of the haze episode; it appeared to be fully aged when the mixing efficiency of NO_3 and SO_4 with BC reached a maximum, i.e., $(NO_3 + SO_4)_{AMS}$ / eBC = ∼ 6. Different from secondary inorganic species, the peak area ratio of (OC + Metal) / C_n showed a high dependence on the mass concentration ratio of POA (e.g., the sum of BBOA and FFOA in BJ, and the sum of BBOA, CCOA, and HOA in GC) to eBC at both sites. These results indicated that the primary OA (POA) co-emitted with BC was more easily internally mixed with BC than secondary inorganic components (e.g., SO_4 and NO_3), although the mass concentration was much lower than that of secondary inorganic aerosol at both the urban and rural sites. Moreover, the mass concentration ratio of secondary organic aerosol (SOA) to eBC also presented a high correlation with (OC + Metal) / C_n in GC ($R^2 = 0.81$) and BJ ($R^2 = 0.95$, Fig. S7). We then used multiple linear regression analysis to quantify the impact of POA and SOA on OC coated on BC. Our results showed that the average contribution of SOA to the coated-OC was nearly twice that of POA (65 % vs. 35 %) in BJ, while POA and SOA contributed similarly in GC.

Figure 4c and d show the relationship between E_{abs} and the ratio of mixing materials to C_n in BJ and GC, respectively. The light absorption enhancement showed a strong dependence on $(NO_3 + SO_4) / C_n$ at both sites. Previous studies found that SOA played an important role in the BC absorption enhancement (Liu et al., 2019b), whereas in our study, the changes in E_{abs} seemed to be independent of (OC + metal) / C_n, likely because (OC + metal) / C_n was influenced by both primary and secondary factors. As shown in Fig. 4c, the ratio of (OC + Metal) / C_n still presented high values at E_{abs} =∼ 1, while the secondary species coated on BC were negligible. These results suggest that OC and metals likely either filled internal void spaces of fresh BC or mainly partly mixed with BC, which did not induce light absorption enhancement at the urban site. With the progress of aging, E_{abs} increased significantly mainly due to the increased secondary coating materials. Similar to BJ, E_{abs} also increased significantly as a function of $(NO_3 + SO_4) / C_n$ in GC. The difference is the high background E_{abs} of ∼ 1.20 in GC when the $(NO_3 + SO_4) / C_n$ ratio was close to 0. A previous study showed that E_{abs} is > 1 when the non-BC material is sufficient to encapsulate the BC (Liu et al., 2017). Considering the peak area ratio of (OC + Metal) / C_n was ∼ 2.5, we inferred that OC and metals were not only filler materials, but also likely coated on fresh BC and induced light absorption enhancement at the rural site. After the further aging process in the atmosphere, E_{abs} was mainly due to the increased secondary inorganic components coated on BC. Moreover, we predicted the E_{abs} using the statistical equations in Fig. 4, with aerosol species measured by AMS. We found that the estimated E_{abs} showed overall agreements with the measured values in both BJ and GC. Although the correlation was not significant (Fig. S8), the average measured and estimated E_{abs} values were similar; these are 1.21 (±0.12) and 1.22 (±0.18) respectively in BJ, and 1.31 (±0.15) and 1.25 (±0.07) respectively in GC. Also, the uncertainty between measurements and predictions was overall below 10 % in both BJ and GC, indicating that the approach is reasonably efficient to estimate E_{abs}. We also estimated the E_{abs} in summer 2017 using the same method. We compared the measurements with a cavity attenuated phase shift single-scattering albedo monitor coupled with a thermodenuder (Fig. S9). Our results showed that the average E_{abs} in summer was 1.24, which was close to the average of about 1.2 reported by Liu et al. (2019a), yet lower than that in Xie et al. (2019a).

3.4 Effects of mixing states on E_{abs}

The PMF analysis is used to characterize the effects of different mixing states on E_{abs}. Five and four factors were identified in BJ and GC, respectively, to elaborate the influence of different mixing states on E_{abs} (Fig. 5). Note that E_{abs} was not estimated when the factor contributed negligibly to the total BC, such as Factor5 in BJ (Fig. 5e). As illustrated in Fig. 5b, Factor2 is the major type of aged BC in the urban region, accounting for more than 60 % of the total BC. This factor was dominated by BC_N, $BCOC_N$, $BCOC_{NS}$, and BC_{NS}, and presented a high E_{abs} of 1.38. Comparatively, FactorB (Fig. 5g) is the major type of aged BC in the rural area, which is dominated by $BCOC_N$. The E_{abs} was ∼ 1.35 for this factor, which was comparable to that in BJ. As this factor evolved towards FactorA (Fig. 5f) after further aging and became internally mixed with a large amount of sulfate, E_{abs} was increased up to 1.41. In BJ, relatively fresh traffic emissions are dominant in Factor4 (Fig. 5d), which showed a negligible impact on light absorption enhancement (∼ 1.06), consistent with results in previous studies (Liu et al., 2017; Sun et al., 2021). Compared with traffic emissions, the relatively fresh biomass burning (Fig. 5c), comprising mainly Mix_{Source} and $BCOC_S$, showed a moderate E_{abs} (∼ 1.11) in BJ. Although the mixed fresh primary emissions (Fig. 5i) in GC presented a relatively low E_{abs} (1.06), we found that the FactorC from coal combustion emissions, mixed with much OC and nitrate, showed a much higher E_{abs} (∼ 1.31) (Fig. 5h). After aging, more sulfate could internally be mixed with BC and enhance the E_{abs}, such as Factor1 (Fig. 5a) with

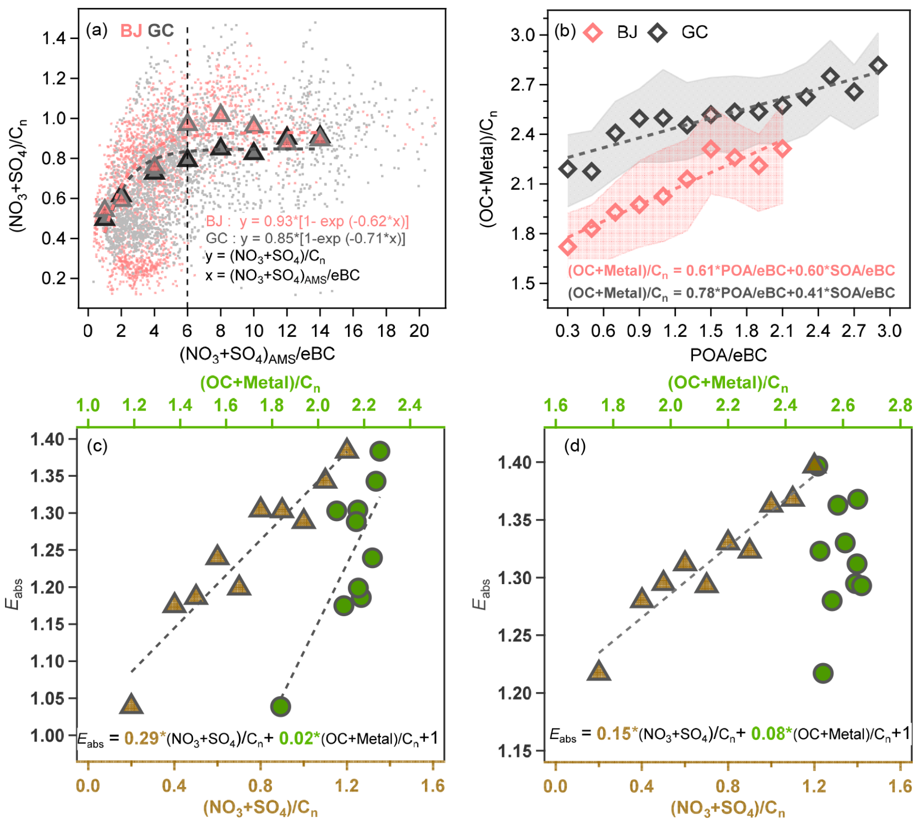

Figure 4. Relationships between peak area ratios and mass concentration ratios **(a)** $(NO_3 + SO_4) / C_n$ vs. $(NO_3 + SO_4)_{AMS} / eBC$ and **(b)** $(OC + Metal) / C_n$ vs. POA / eBC. Relationships between E_{abs} and peak area ratios of coating materials $(NO_3 + SO_4) / C_n$ and $(OC + Metal) / C_n$ in **(c)** Beijing and **(d)** Gucheng. The triangles in **(a)** are the averages of different bins grouped according to $(NO_3 + SO_4)_{AMS} / eBC$. The rhombuses in **(b)** are the averages of different bins that are grouped according to POA / eBC. The shaded areas in **(b)** indicate the 25th and 75th percentiles of the $(OC + Metal) / C_n$ ratios. The triangles and circles in **(c)** and **(d)** are the averages of different bins grouped according to $(NO_3 + SO_4) / C_n$.

E_{abs} up to 1.42. Overall, E_{abs} shows a similar dependence on the evolution of the mixing state of BC-containing particles at urban and rural sites; i.e., fresh BC particles from primary emissions (e.g., biomass burning and traffic) showed a small E_{abs} (1.06–1.11). At a relatively high RH level, BC could be directly mixed with nitrate or OC–nitrate (BC_N and $BCOC_N$), accounting for more than 60 % of BC (mass concentration), and lead to an increase in E_{abs} above 1.30. Then, the BC-containing particles were further mixed with sulfate (BC_{NS} and $BCOC_{NS}$) after continuous aging in the atmosphere, and resulted in the highest E_{abs} above 1.40.

Based on E_{abs} for each factor and its contribution to $b_{abs,\,BCpure}$, we estimated the direct radiative forcing (ΔF_R) caused by pure BC at the top of the atmosphere (TOA), and the absorption ΔF_R enhanced by the mixed state of BC-containing particles (Chylek and Wong, 1995; Chen and Bond, 2010). The detailed descriptions for the estimation are presented in the Supplement. It should be noted that BrC can also absorb light at 870 nm, leading to an overestimation of BC absorption. Considering that the contribution of BrC to the total absorption at 870 nm is typically small (< 1 %) (Clarke et al., 2004; Fialho et al., 2005; Yang et al., 2009), the impact of BrC on the estimation of the radiative forcing of BC is expected to be small as well. As shown in Fig. 5, the ΔF_R caused by pure BC particles is about +0.43 and +0.60 $W\,m^{-2}$ in Beijing and Gucheng, respectively. Considering the mixing state of BC, ΔF_R could increase to 0.59 and 0.82 $W\,m^{-2}$ in Beijing and Gucheng, respectively. Our results demonstrate that the mixing state of BC-containing particles can have a large impact on the radiative forcing estimation, by up to 27 %.

4 Conclusions

HR-SPAMS, TD-PAX, and HR-AMS were deployed at the urban and rural sites in the North China Plain in winter 2019, to characterize the chemical composition and mixing state of BC-containing particles and their impact on light absorption enhancement. Our results showed that BC-containing particles were primarily mixed with OC, NO_3, and SO_4 at both sites, while the rural site showed a much higher fraction of OC- and nitrate-coated BC (36 % vs. 15 %–20%). The in-

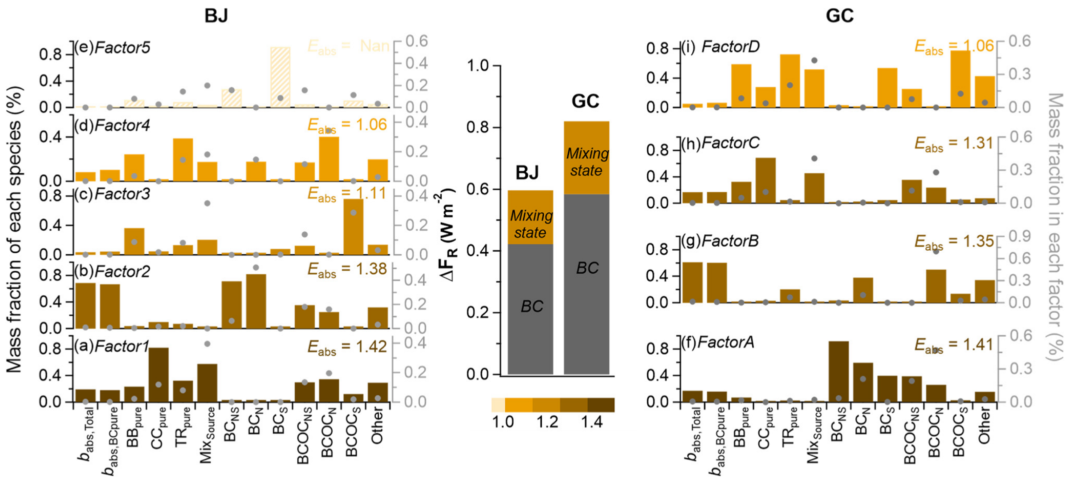

Figure 5. Factor profiles and their contributions to each factor identified by the positive matrix factorization model in Beijing and Gucheng. $b_{abs,\,total}$ and $b_{abs,\,BCpure}$ represent light absorption ($M\,m^{-1}$) of coated BC particles and pure BC, respectively. BC types, e.g., BB_{pure}, in counted units.

creased BC particles internally mixed with a large amount of NO_3 were mainly due to the effect of the clean air action that reduced much more sulfate than nitrate in $PM_{2.5}$. The average contribution of SOA to the OC coated on BC was about twice that of POA in BJ, while both of them contributed similarly to the OC coating in GC. In addition, OC and metals were likely filler materials internally mixed with fresh BC, and did not induce much light absorption enhancement at the urban site; however, they were coated on fresh BC and induced light absorption enhancement (~ 1.2) at the rural site.

By analyzing the variations of the BC mixing state in different environments, we found that BC particles were primarily mixed with NO_3, with an increase of RH at both the urban and rural sites. In particular, the BC emitted from biomass burning was first mixed with NO_3 at a relatively high RH level, and then mixed with both nitrate and sulfate after further aging. Comparatively, the BC emitted from coal combustion was more internally mixed with OC and NO_3, and then mixed with sulfate ($BCOC_{NS}$) with similar processes. Thus, high coal combustion emissions can result in the increase of the $BCOC_N$ fraction with the increase of RH at the rural site, while BC_N was generally the dominant BC-containing particle type in Beijing. Although BC particles presented a different mixing state in different environments, E_{abs} showed a similar evolutionary dependence on the changes in mixing states, i.e., from the small E_{abs} (1.06–1.11) with fresh BC emissions, to above 1.30 after aging and internal mixing with nitrate and OC–nitrate (BC_N and $BCOC_N$), and to above 1.40 after further aging with the sulfate involved.

Data availability. The data in this study are available from the authors upon request (sunyele@mail.iap.ac.cn).

Supplement. The supplement related to this article is available online at: https://doi.org/10.5194/acp-22-7619-2022-supplement.

Author contributions. YS and JS designed the research. JS, CX, WX, CC and ZL conducted the measurements. JS, WX, CC, ZhW and YL analyzed the data. CX, LL, XD, FH, XP, NM, WX, PF and ZiW reviewed and commented on the paper. JS and YS wrote the paper.

Competing interests. The contact author has declared that neither they nor their co-authors have any competing interests.

Disclaimer. Publisher's note: Copernicus Publications remains neutral with regard to jurisdictional claims in published maps and institutional affiliations.

Financial support. This work was supported by the National Natural Science Foundation of China (grant nos. 9204430003 and 42061134008).

Review statement. This paper was edited by Willy Maenhaut and reviewed by three anonymous referees.

References

Bi, X. H., Dai, S. H., Zhang, G. H., Qiu, N., Li, M., Wang, X. M., Chen, D. H., Peng, P. A., Sheng, G. Y., Fu, J. M., and Zhou, Z.: Real-time and single-particle volatility of elemental carbon containing particles in the urban area of Pearl River Delta region, China, Atmos. Environ., 118, 194–202, https://doi.org/10.1016/j.atmosenv.2015.08.012, 2015.

Bond, T. C. and Bergstrom, R. W.: Light absorption by carbonaceous particles: an investigative review, Aerosol Sci. Tech., 40, 27–67, https://doi.org/10.1080/02786820500421521, 2006.

Bond, T. C., Doherty, S. J., Fahey, D. W., Forster, P. M., Berntsen, T., DeAngelo, B. J., Flanner, M. G., Ghan, S., Kärcher, B., Koch, D., Kinne, S., Kondo, Y., Quinn, P. K., Sarofim, M. C., Schultz, M. G., Schulz, M., Venkataraman, C., Zhang, H., Zhang, S., Bellouin, N., Guttikunda, S. K., Hopke, P. K., Jacobson, M. Z., Kaiser, J. W., Klimont, Z., Lohmann, U., P., S. J., Shindell, D., Storelvmo, T., Warren, S. G., and Zender, C. S.: Bounding the role of black carbon in the climate system: a scientific assessment, J. Geophys. Res.-Atmos., 118, 5380–5552, https://doi.org/10.1002/jgrd.50171, 2013.

Buseck, P. R., Adachi, K., Andras, G., Tompa, E., and Mihaly, P.: Ns-Soot: a material-based term for strongly light-absorbing carbonaceous particles, Aerosol Sci. Tech., 48, 777–788, https://doi.org/10.1080/02786826.2014.919374, 2014.

Cappa, C. D., Onasch, T. B., Massoli, P., Worsnop, D. R., Bates, T. S., Cross, E. S., Davidovits, P., Hakala, J., Hayden, K. L., and Jobson, B. T.: Radiative absorption enhancements due to the mixing state of atmospheric black carbon, Science, 337, 1078–1081, https://doi.org/10.1126/science.1223447, 2012.

Cappa, C. D., Zhang, X., Russell, L. M., Collier, S., Lee, A. K. Y., Chen, C.-L., Betha, R., Chen, S., Liu, J., Price, D. J., Sanchez, K. J., McMeeking, G. R., Williams, L. R., Onasch, T. B., Worsnop, D. R., Abbatt, J., and Zhang, Q.: Light absorption by ambient black and brown carbon and its dependence on black carbon coating state for two California, USA, cities in winter and summer, J. Geophys. Res.-Atmos., 124, 1550–1577, https://doi.org/10.1029/2018jd029501, 2019.

Chen, C., Qiu, Y., Weiqi, X., He, Y., Li, Z., Sun, J., Ma, N., Xu, W., Pan, X., Fu, P., Wang, Z., and Sun, Y.: Primary emissions and secondary aerosol processing during wintertime in rural area of North China Plain, J. Geophys. Res.-Atmos., 127, e2021JD035430, https://doi.org/10.1029/2021JD035430, 2022.

Chen, L., Zhang, F., Yan, P., Wang, X., Sun, L., Li, Y., Zhang, X., Sun, Y., and Li, Z.: The large proportion of black carbon (BC)-containing aerosols in the urban atmosphere, Environ. Pollut., 263, 114507, https://doi.org/10.1016/j.envpol.2020.114507, 2020.

Chen, Y. and Bond, T. C.: Light absorption by organic carbon from wood combustion, Atmos. Chem. Phys., 10, 1773–1787, https://doi.org/10.5194/acp-10-1773-2010, 2010.

Chen, Y., Cao, J., Huang, R., Yang, F., Wang, Q., and Wang, Y.: Characterization, mixing state, and evolution of urban single particles in Xi'an (China) during wintertime haze days, Sci. Total Environ., 573, 937–945, https://doi.org/10.1016/j.scitotenv.2016.08.151, 2016.

Chen, Y., Tian, M., Huang, R.-J., Shi, G., Wang, H., Peng, C., Cao, J., Wang, Q., Zhang, S., Guo, D., Zhang, L., and Yang, F.: Characterization of urban amine-containing particles in southwestern China: seasonal variation, source, and processing, Atmos. Chem. Phys., 19, 3245–3255, https://doi.org/10.5194/acp-19-3245-2019, 2019.

Chen, Y., Cai, J., Wang, Z., Peng, C., Yao, X., Tian, M., Han, Y., Shi, G., Shi, Z., Liu, Y., Yang, X., Zheng, M., Zhu, T., He, K., Zhang, Q., and Yang, F.: Simultaneous measurements of urban and rural particles in Beijing – Part 1: Chemical composition and mixing state, Atmos. Chem. Phys., 20, 9231–9247, https://doi.org/10.5194/acp-20-9231-2020, 2020a.

Chen, Y., Kozlovskiy, V., Du, X., Lv, J., Nikiforov, S., Yu, J., Kolosov, A., Gao, W., Zhou, Z., Huang, Z., and Li, L.: Increase of the particle hit rate in a laser single-particle mass spectrometer by pulse delayed extraction technology, Atmos. Meas. Tech., 13, 941–949, https://doi.org/10.5194/amt-13-941-2020, 2020b.

Chylek, P. and Wong, J.: Effect of aerosols on global budget, Geophys. Res. Lett., 22, 929–931, 1995.

Clarke, A. D., Shinozuka, Y., Kapustin, V. N., Howell, S., Huebert, B., Doherty, S., Anderson, T., Covert, D., Anderson, J., Hua, X., Moore, K. G., McNaughton, C., Carmichael, G., and Weber, R.: Size distributions and mixtures of dust and black carbon aerosol in Asian outflow: physiochemistry and optical properties, J. Geophys. Res.-Atmos., 109, e2003jd004378, https://doi.org/10.1029/2003jd004378, 2004.

Ding, A. J., Huang, X., Nie, W., Sun, J. N., Kerminen, V. M., Petäjä, T., Su, H., Cheng, Y. F., Yang, X. Q., Wang, M. H., Chi, X. G., Wang, J. P., Virkkula, A., Guo, W. D., Yuan, J., Wang, S. Y., Zhang, R. J., Wu, Y. F., Song, Y., Zhu, T., Zilitinkevich, S., Kulmala, M., and Fu, C. B.: Enhanced haze pollution by black carbon in megacities in China, Geophys. Res. Lett., 43, 2873–2879, https://doi.org/10.1002/2016gl067745, 2016.

Ding, S., Liu, D., Hu, K., Zhao, D., Tian, P., Wang, F., Li, R., Chen, Y., He, H., Huang, M., and Ding, D.: Optical and hygroscopic properties of black carbon influenced by particle microphysics at the top of the anthropogenically polluted boundary layer, Atmos. Chem. Phys., 21, 681–694, https://doi.org/10.5194/acp-21-681-2021, 2021.

Fialho, P., Hansen, A. D. A., and Honrath, R. E.: Absorption coefficients by aerosols in remote areas: a new approach to decouple dust and black carbon absorption coefficients using seven-wavelength Aethalometer data, J. Aerosol. Sci., 36, 267–282, https://doi.org/10.1016/j.jaerosci.2004.09.004, 2005.

Fuller, K. A., Malm, W. C., and Kreidenweis, S. M.: Effects of mixing on extinction by carbonaceous particles, J. Geophys. Res., 104, 15941–15954, https://doi.org/10.1029/1998jd100069, 1999.

Healy, R. M., Hellebust, S., Kourtchev, I., Allanic, A., O'Connor, I. P., Bell, J. M., Healy, D. A., Sodeau, J. R., and Wenger, J. C.: Source apportionment of $PM_{2.5}$ in Cork Harbour, Ireland using a combination of single particle mass spectrometry and quantitative semi-continuous measurements, Atmos. Chem. Phys., 10, 9593–9613, https://doi.org/10.5194/acp-10-9593-2010, 2010.

Healy, R. M., Sciare, J., Poulain, L., Kamili, K., Merkel, M., Müller, T., Wiedensohler, A., Eckhardt, S., Stohl, A., Sarda-Estève, R., McGillicuddy, E., O'Connor, I. P., Sodeau, J. R., and Wenger, J. C.: Sources and mixing state of size-resolved elemental carbon particles in a European megacity: Paris, Atmos. Chem. Phys., 12, 1681–1700, https://doi.org/10.5194/acp-12-1681-2012, 2012.

IPCC: Climate Change 2013: The Physical Science Basis. Contribution of Working Group I to the Fifth Assessment Report of the Intergovernmental Panel on Climate Change, edited by: Stocker, T. F., Qin, D., Plattner, G.-K., Tignor, M., Allen, S. K., Boschung, J., Nauels, A., Xia, Y., Bex, V., and Midgley, P. M., Cambridge University Press, Cambridge, United Kingdom and New York, NY, USA, 1535 pp., https://doi.org/10.1017/CBO9781107415324, 2013.

Kahnert, M.: On the discrepancy between modeled and measured mass absorption cross sections of light absorbing carbon aerosols, Aerosol Sci. Tech., 44, 453–460, https://doi.org/10.1080/02786821003733834, 2010.

Lack, D. A. and Cappa, C. D.: Impact of brown and clear carbon on light absorption enhancement, single scatter albedo and absorption wavelength dependence of black carbon, Atmos. Chem. Phys., 10, 4207–4220, https://doi.org/10.5194/acp-10-4207-2010, 2010.

Lee, A. K. Y., Willis, M. D., Healy, R. M., Onasch, T. B., and Abbatt, J. P. D.: Mixing state of carbonaceous aerosol in an urban environment: single particle characterization using the soot particle aerosol mass spectrometer (SP-AMS), Atmos. Chem. Phys., 15, 1823–1841, https://doi.org/10.5194/acp-15-1823-2015, 2015.

Lei, L., Zhou, W., Chen, C., He, Y., Li, Z., Sun, J., Tang, X., Fu, P., Wang, Z., and Sun, Y.: Long-term characterization of aerosol chemistry in cold season from 2013 to 2020 in Beijing, China, Environ. Pollut., 268, 115952, https://doi.org/10.1016/j.envpol.2020.115952, 2020.

Li, L., Huang, Z., Dong, J., Li, M., Gao, W., Nian, H., Fu, Z., Zhang, G., Bi, X., Cheng, P., and Zhou, Z.: Real time bipolar time-of-flight mass spectrometer for analyzing single aerosol particles, Int. J. Mass Spectrom., 303, 118–124, https://doi.org/10.1016/j.ijms.2011.01.017, 2011.

Li, W., Sun, J., Xu, L., Shi, Z., Riemer, N., Sun, Y., Fu, P., Zhang, J., Lin, Y., Wang, X., Shao, L., Chen, J., Zhang, X., Wang, Z., and Wang, W.: A conceptual framework for mixing structures in individual aerosol particles, J. Geophys. Res.-Atmos., 121, 13784–13798, https://doi.org/10.1002/2016jd025252, 2016.

Li, W. J., Shao, L. Y., Zhang, D. Z., Ro, C. U., Hu, M., Bi, X. H., Geng, H., Matsuki, A., Niu, H. Y., and Chen, J. M.: A review of single aerosol particle studies in the atmosphere of East Asia: morphology, mixing state, source, and heterogeneous reactions, J. Clean Prod., 112, 1330–1349, https://doi.org/10.1016/j.jclepro.2015.04.050, 2016.

Liu, D., Whitehead, J., Alfarra, M. R., Reyes-Villegas, E., Spracklen, D. V., Reddington, C. L., Kong, S., Williams, P. I., Ting, Y.-C., Haslett, S., Taylor, J. W., Flynn, M. J., Morgan, W. T., McFiggans, G., Coe, H., and Allan, J. D.: Black-carbon absorption enhancement in the atmosphere determined by particle mixing state, Nat. Geosci., 10, 184–188, https://doi.org/10.1038/ngeo2901, 2017.

Liu, D., Joshi, R., Wang, J., Yu, C., Allan, J. D., Coe, H., Flynn, M. J., Xie, C., Lee, J., Squires, F., Kotthaus, S., Grimmond, S., Ge, X., Sun, Y., and Fu, P.: Contrasting physical properties of black carbon in urban Beijing between winter and summer, Atmos. Chem. Phys., 19, 6749–6769, https://doi.org/10.5194/acp-19-6749-2019, 2019a.

Liu, D., Zhao, D., Xie, Z., Yu, C., Chen, Y., Tian, P., Ding, S., Hu, K., Lowe, D., Liu, Q., Zhou, W., Wang, F., Sheng, J., Kong, S., Hu, D., Wang, Z., Huang, M., and Ding, D.: Enhanced heating rate of black carbon above the planetary boundary layer over megacities in summertime, Environ. Res. Lett., 14, 124003, https://doi.org/10.1088/1748-9326/ab4872, 2019b.

Liu, D., Ding, S., Zhao, D., Hu, K., Yu, C., Hu, D., Wu, Y., Zhou, C., Tian, P., Liu, Q., Wu, Y., Zhang, J., Kong, S., Huang, M., and Ding, D.: Black carbon emission and wet scavenging from surface to the top of boundary layer over Beijing region, J. Geophys. Res.-Atmos., 125, e2020JD033096, https://doi.org/10.1029/2020jd033096, 2020.

Liu, S., Aiken, A. C., Gorkowski, K., Dubey, M. K., Cappa, C. D., Williams, L. R., Herndon, S. C., Massoli, P., Fortner, E., and Chhabra, P. S.: Enhanced light absorption by mixed source black and brown carbon particles in UK winter, Nat. Commun., 6, 8435–8435, https://doi.org/10.1080/02786820500421521, 2015.

Ma, Y., Huang, C., Jabbour, H., Zheng, Z., Wang, Y., Jiang, Y., Zhu, W., Ge, X., Collier, S., and Zheng, J.: Mixing state and light absorption enhancement of black carbon aerosols in summertime Nanjing, China, Atmos. Environ., 222, 117141, https://doi.org/10.1016/j.atmosenv.2019.117141, 2020.

Petit, J.-E., Favez, O., Sciare, J., Canonaco, F., Croteau, P., Močnik, G., Jayne, J., Worsnop, D., and Leoz-Garziandia, E.: Submicron aerosol source apportionment of wintertime pollution in Paris, France by double positive matrix factorization (PMF^2) using an aerosol chemical speciation monitor (ACSM) and a multi-wavelength Aethalometer, Atmos. Chem. Phys., 14, 13773–13787, https://doi.org/10.5194/acp-14-13773-2014, 2014.

Pratt, K. A. and Prather, K. A.: Mass spectrometry of atmospheric aerosols-recent developments and applications. Part II: on-line mass spectrometry techniques, Mass Spectrom. Rev., 31, 17–48, https://doi.org/10.1002/mas.20330, 2012.

Shen, W., Dai, X., Huang, Z., Hou, Z., Cai, W., Du, X., Zhou, Z., Li, M., and Li, L.: Improvement of the dynamic range of data acquisition system in single particle mass spectrometry, J. Chinese Cinemas., 039, 331–336, 2018.

Silva, P. J., Liu, D. Y., Noble, C. A., and Prather, K. A.: Size and chemical characterization of individual particles resulting from biomass burning of local Southern California species, Environ. Sci. Technol., 33, 3068–3076, https://doi.org/10.1021/es980544p, 1999.

Song, X. H., Hopke, P. K., Fergenson, D. P., and Prather, K. A.: Classification of single particles analyzed by ATOFMS using an artificial neural network, ART-2A, Anal. Chem., 71, 860–865, https://doi.org/10.1021/ac9809682, 1999.

Sun, J., Xie, C., Xu, W., Chen, C., Ma, N., Xu, W., Lei, L., Li, Z., He, Y., Qiu, Y., Wang, Q., Pan, X., Su, H., Cheng, Y., Wu, C., Fu, P., Wang, Z., and Sun, Y.: Light absorption of black carbon and brown carbon in winter in North China Plain: comparisons between urban and rural sites, Sci. Total Environ., 770, 144821, https://doi.org/10.1016/j.scitotenv.2020.144821, 2021.

Sun, J., Wang, Z., Zhou, W., Xie, C., Wu, C., Chen, C., Han, T., Wang, Q., Li, Z., Li, J., Fu, P., Wang, Z., and Sun, Y.: Measurement report: Long-term changes in black carbon and aerosol optical properties from 2012 to 2020 in Beijing, China, Atmos. Chem. Phys., 22, 561–575, https://doi.org/10.5194/acp-22-561-2022, 2022.

Sun, Y., Wang, Z., Wild, O., Xu, W., Chen, C., Fu, P., Du, W., Zhou, L., Zhang, Q., Han, T., Wang, Q., Pan, X., Zheng, H., Li, J., Guo, X., Liu, J., and Worsnop, D. R.: “APEC Blue”: secondary aerosol reductions from emission controls in Beijing, Sci. Rep.-UK, 6, 20668, https://doi.org/10.1038/srep20668, 2016.

Sun, Y., He, Y., Kuang, Y., Xu, W., Song, S., Ma, N., Tao, J., Cheng, P., Wu, C., Su, H., Cheng, Y., Xie, C., Chen, C., Lei, L., Qiu, Y., Fu, P., Croteau, P., and Worsnop, D. R.: Chemical differences between PM_1 and $PM_{2.5}$ in highly polluted environment and implications in air pollution studies, Geophys. Res. Lett., 47, e2019GL086288, https://doi.org/10.1029/2019gl086288, 2020.

Thamban, N. M., Tripathi, S. N., Moosakutty, S. P., Kuntamukkala, P., and Kanawade, V. P.: Internally mixed black carbon in the Indo-Gangetic Plain and its effect on absorption enhancement, Atmos. Res., 197, 211–223, https://doi.org/10.1016/j.atmosres.2017.07.007, 2017.

Vignati, E., Karl, M., Krol, M., Wilson, J., Stier, P., and Cavalli, F.: Sources of uncertainties in modelling black carbon at the global scale, Atmos. Chem. Phys., 10, 2595–2611, https://doi.org/10.5194/acp-10-2595-2010, 2010.

Wang, Q., Cao, J., Han, Y., Wang, G., Li, G., Wang, Y., Dai, W., Zhang, R., Zhou, Y., and Psi, V.: Mixing state of black carbon aerosol in a heavily polluted urban area of China: implications for light absorption enhancement, Aerosol Sci. Tech., 48, 689–697, 2014.

Wang, Q., Li, L., Zhou, J., Ye, J., Dai, W., Liu, H., Zhang, Y., Zhang, R., Tian, J., Chen, Y., Wu, Y., Ran, W., and Cao, J.: Measurement report: Source and mixing state of black carbon aerosol in the North China Plain: implications for radiative effect, Atmos. Chem. Phys., 20, 15427–15442, https://doi.org/10.5194/acp-20-15427-2020, 2020.

Xie, C., Xu, W., Wang, J., Liu, D., Ge, X., Zhang, Q., Wang, Q., Du, W., Zhao, J., and Zhou, W.: Light absorption enhancement of black carbon in urban Beijing in summer, Atmos. Environ., 213, 499–504, 2019a.

Xie, C., Xu, W., Wang, J., Wang, Q., Liu, D., Tang, G., Chen, P., Du, W., Zhao, J., Zhang, Y., Zhou, W., Han, T., Bian, Q., Li, J., Fu, P., Wang, Z., Ge, X., Allan, J., Coe, H., and Sun, Y.: Vertical characterization of aerosol optical properties and brown carbon in winter in urban Beijing, China, Atmos. Chem. Phys., 19, 165–179, https://doi.org/10.5194/acp-19-165-2019, 2019b.

Xie, C., He, Y., Lei, L., Zhou, W., Liu, J., Wang, Q., Xu, W., Qiu, Y., Zhao, J., Sun, J., Li, L., Li, M., Zhou, Z., Fu, P., Wang, Z., and Sun, Y.: Contrasting mixing state of black carbon-containing particles in summer and winter in Beijing, Environ. Pollut., 263, 114455, https://doi.org/10.1016/j.envpol.2020.114455, 2020.

Xu, W., Chen, C., Qiu, Y., Li, Y., Zhang, Z., Karnezi, E., Pandis, S. N., Xie, C., Li, Z., Sun, J., Ma, N., Xu, W., Fu, P., Wang, Z., Zhu, J., Worsnop, D. R., Ng, N. L., and Sun, Y.: Organic aerosol volatility and viscosity in the North China Plain: contrast between summer and winter, Atmos. Chem. Phys., 21, 5463–5476, https://doi.org/10.5194/acp-21-5463-2021, 2021a.

Xu, W., Chen, C., Qiu, Y., Xie, C., Chen, Y., Ma, N., Xu, W., Fu, P., Wang, Z., Pan, X., Zhu, J., Ng, N. L., and Sun, Y.: Size-resolved characterization of organic aerosol in the North China Plain: new insights from high resolution spectral analysis, Environ. Sci.: Atmos., 1, 346–358, https://doi.org/10.1039/d1ea00025j, 2021b.

Yang, J., Ma, S., Gao, B., Li, X., Zhang, Y., Cai, J., Li, M., Yao, L., Huang, B., and Zheng, M.: Single particle mass spectral signatures from vehicle exhaust particles and the source apportionment of on-line $PM_{2.5}$ by single particle aerosol mass spectrometry, Sci. Total Environ., 593, 310–318, https://doi.org/10.1016/j.scitotenv.2017.03.099, 2017.

Yang, M., Howell, S. G., Zhuang, J., and Huebert, B. J.: Attribution of aerosol light absorption to black carbon, brown carbon, and dust in China – interpretations of atmospheric measurements during EAST-AIRE, Atmos. Chem. Phys., 9, 2035–2050, https://doi.org/10.5194/acp-9-2035-2009, 2009.

Zhang, G., Bi, X., Chan, L. Y., Li, L., Wang, X., Feng, J., Sheng, G., Fu, J., Li, M., and Zhou, Z.: Enhanced trimethylamine-containing particles during fog events detected by single particle aerosol mass spectrometry in urban Guangzhou, China, Atmos. Environ., 55, 121–126, https://doi.org/10.1016/j.atmosenv.2012.03.038, 2012.

Zhang, Q., Zheng, Y., Tong, D., Shao, M., Wang, S., Zhang, Y., Xu, X., Wang, J., He, H., Liu, W., Ding, Y., Lei, Y., Li, J., Wang, Z., Zhang, X., Wang, Y., Cheng, J., Liu, Y., Shi, Q., Yan, L., Geng, G., Hong, C., Li, M., Liu, F., Zheng, B., Cao, J., Ding, A., Gao, J., Fu, Q., Huo, J., Liu, B., Liu, Z., Yang, F., He, K., and Hao, J.: Drivers of improved $PM_{2.5}$ air quality in China from 2013 to 2017, P. Natl. Acad. Sci. USA, 116, 24463–24469, https://doi.org/10.1073/pnas.1907956116, 2019.

Zhang, X., Kim, H., Parworth, C. L., Young, D. E., Zhang, Q., Metcalf, A. R., and Cappa, C. D.: Optical properties of wintertime aerosols from residential wood burning in Fresno, CA: results from DISCOVER-AQ 2013, Environ. Sci. Technol., 50, 1681–1690, https://doi.org/10.1021/acs.est.5b04134, 2016.

Zhang, Y., Wang, X., Chen, H., Yang, X., Chen, J., and Allen, J. O.: Source apportionment of lead-containing aerosol particles in Shanghai using single particle mass spectrometry, Chemosphere, 74, 501–507, https://doi.org/10.1016/j.chemosphere.2008.10.004, 2009.

Zhang, Y., Favez, O., Canonaco, F., Liu, D., Močnik, G., Amodeo, T., Sciare, J., Prévôt, A. S. H., Gros, V., and Albinet, A.: Evidence of major secondary organic aerosol contribution to lensing effect black carbon absorption enhancement, npj Clim. Atmos. Sci., 1, 1–8, https://doi.org/10.1038/s41612-018-0056-2, 2018.

Zhang, Y., Liu, H., Lei, S., Xu, W., Tian, Y., Yao, W., Liu, X., Liao, Q., Li, J., Chen, C., Sun, Y., Fu, P., Xin, J., Cao, J., Pan, X., and Wang, Z.: Mixing state of refractory black carbon in fog and haze at rural sites in winter on the North China Plain, Atmos. Chem. Phys., 21, 17631–17648, https://doi.org/10.5194/acp-21-17631-2021, 2021.

Zhong, Q. E., Cheng, C., Wang, Z., Li, L., Li, M., Ge, D., Wang, L., Li, Y., Nie, W., Chi, X., Ding, A., Yang, S., Chen, D., and Zhou, Z.: Diverse mixing states of amine-containing single particles in Nanjing, China, Atmos. Chem. Phys., 21, 17953–17967, https://doi.org/10.5194/acp-21-17953-2021, 2021.

Zhou, W., Gao, M., He, Y., Wang, Q., Xie, C., Xu, W., Zhao, J., Du, W., Qiu, Y., Lei, L., Fu, P., Wang, Z., Worsnop, D. R., Zhang, Q., and Sun, Y.: Response of aerosol chemistry to clean air action in Beijing, China: insights from two-year ACSM measurements and model simulations, Environ. Pollut., 255, 113345, https://doi.org/10.1016/j.envpol.2019.113345, 2019.

Zhu, S., Li, L., Wang, S., Li, M., Liu, Y., Lu, X., Chen, H., Wang, L., Chen, J., Zhou, Z., Yang, X., and Wang, X.: Development of an automatic linear calibration method for high-resolution single-particle mass spectrometry: improved chemical species identification for atmospheric aerosols, Atmos. Meas. Tech., 13, 4111–4121, https://doi.org/10.5194/amt-13-4111-2020, 2020.